Analytical Letters

ISSN: 0003-2719 (Print) 1532-236X (Online) Journal homepage: http://www.tandfonline.com/loi/lanl20

Estimation of Protein Content in Plant Leaves using Spectral Reflectance: A Case Study in Euonymus japonica

Xing Yan , Wenzhong Shi , Wenji Zhao & Nana Luo

To cite this article: Xing Yan , Wenzhong Shi , Wenji Zhao & Nana Luo (2014) Estimation of Protein Content in Plant Leaves using Spectral Reflectance: A Case Study in Euonymus japonica , Analytical Letters, 47:3, 517-530, DOI: 10.1080/00032719.2013.843187

To link to this article: http://dx.doi.org/10.1080/00032719.2013.843187

Analytical Letters, 47: 517–530, 2014

ISSN: 0003-2719 print/1532-236X online
DOI: 10.1080/00032719.2013.843187

Taylor & Francis
Taylor & Francis Group

Spectroscopy

ESTIMATION OF PROTEIN CONTENT IN PLANT LEAVES USING SPECTRAL REFLECTANCE: A CASE STUDY IN *EUONYMUS JAPONICA*

Xing Yan,[1] Wenzhong Shi,[1] Wenji Zhao,[2] and Nana Luo[2]
[1]*The Department of Land Surveying and Geo-Informatics, The Hong Kong Polytechnic University, Hong Kong, China*
[2]*College of Resource Environment and Tourism, Capital Normal University, Beijing, China*

Reflectance spectroscopy has been widely applied in the field of environmental studies. In this study, a low-cost, rapid, and nondestructive method using spectral reflectance was explored to evaluate protein concentrations in plant leaves of* Euonymus japonica. *Proteins in leaf samples were extracted and separated by sodium dodecyl sulfate polyacrylamide gel electrophoresis, and five specific protein bands of interest were identified and quantified. Correlation analysis indicated that spectral reflectance had significant relationships with ribulose bisphosphate carboxylase a ($r = -0.43$) and chlorophyll a-b binding protein ($r = 0.53$). A linear regression model and a quadratic regression model were formulated to directly and rapidly estimate the concentration of these two proteins with $R^2 = 0.61$ and 0.7, respectively. To more accurately estimate the concentration of proteins, a precise inversion was established by a back propagation neutral network model using plant spectral absorption and position parameters, and the R^2 values for proteins ribulose bisphosphate carboxylase, chlorophyll a-b binding protein, oxygen evolving enhancer protein, and ATP synthase subunit beta were 0.90, 0.91, 0.91, and 0.93, respectively. The models established in this study were shown to be useful tools for studies of plant biochemical components and health under different environmental conditions.

Keywords: Back propagation neutral networks; Plant leaves; Proteins; Regression model; Spectral reflectance

INTRODUCTION

With the development of industry, environmental pollution has become an increasingly serious problem and a global challenge because some industrial pollutants have the potential to negatively affect plant growth and damage the

Received 7 August 2013; accepted 2 September 2013.

Address correspondence to Wenzhong Shi, The Department of Land Surveying and Geo-Informatics, The Hong Kong Polytechnic University, Hong Kong, China. E-mail: lswzshi@polyu.edu.hk

Color versions of one or more of the figures in the article can be found online at www.tandfonline.com/lanl.

ecological system (Wang and Xie 2009; Sun et al. 2006). To investigate the effects of environmental conditions on plant growth and plant health, different methods have been employed and used (Heim, Tagliaferro, and Bobilya 2002; Chalke 1999; Harbome 1999). In order to analyze the effects of environmental pollution on ecological systems, evaluation of the vegetation growth state can estimate level of damage to the system. Meanwhile, an ideal vegetation parameter should be determined that is highly sensitive to single environmental change and represents plant growth well, such as protein conditions (Hansena, Schjoerring, and Thomsen 2002).

Protein content is an important parameter for vegetation growth as well as for environmental level; thus, many scientists have tried to estimate this parameter (Jenneer, Ugalde, and Aspinall, 1991). Traditional chemical analysis is accurate and reliable for determination of plant physical conditions, but it is time consuming, high cost, and destructive to plants (Blackmer, Schepers, and Vavrel 1996). In addition, this method cannot be used to monitor plant growth dynamically and rapidly over the long term.

Over the last three decades, spectroscopic technology has been widely used for determination of vegetation biochemical indexes such as chlorophyll protein as it is simple and nondamaging for plant (Aparicio et al. 2000; Adams, Philpot, and Norvell 1999; Best and Harlan 1985). Hansena et al. (2002) used repeated canopy reflectance measurements and a partial least squares (PLS) regression model to predict grain yield and protein content. The result showed that spectral data from repeated canopy reflectance measurements with the model improved the prediction accuracy of grain yield and protein content (Hansena et al. 2002). Meanwhile, comparing field spectra with laboratory spectra could successfully estimate foliar nitrogen concentration of heather (Kalaitzidis, Caporn, and Cutler 2008). The nitrogen concentration was calculated through destructive sampling and chemical analysis. Based on the stepwise multiple regression analysis, the waveband closely associated with nitrogen concentration was identified. Further study showed that near-infrared spectroscopy was the ideal method to quantify the nitrogen content of fresh cotton leaves (Markr and Loretoc 2002). Curran, Dungan, and Peterson (2011) also found that reflectance spectroscopy could successfully estimate the foliar biochemical concentrations in ground fresh pine needles (including chlorophyll a, chlorophyll b, total chlorophyll, lignin, nitrogen, cellulose, water, phosphorous, protein, amino acids, sugar, starch) by using stepwise regression theory, which included three methodologies, standard first derivative reflectance spectra, center of the absorption feature, and area of the absorption feature (Curran et al. 2011). Thus, spectral technology provides a rapid and temporal method to predict vegetation proteins. Present reports showed that the correlation between plant protein and spectral reflectance was observed significantly and positively. However, since most of the previous studies focus on the chlorophyll concentration inversion by spectral reflectance, little research on the correlation between spectral reflectance features and different proteins has been conducted. Furthermore, few current studies have made use of spectral reflectance models to directly monitor content of varied plant proteins.

This study focused on the spectral reflectance features of plant leaf surfaces and various inner proteins in *Euonymus japonica*. The objective was to explore a low-cost,

rapid, and nondestructive method to evaluate the protein concentrations in plant and lay a methodological basis for further investigation of plant health.

MATERIALS AND METHODS

Study Area

This study was conducted in the city of Beijing, the capital of China. Beijing lies at east longitude 39.92°, north latitude 116.46° and covers an area of 16,507.5 km^2. It is located at the northern edge of the North China Plain at the junction of Inner Mongolia Plateau, Loess Plateau and North China Plain.

Plant Materials

Euonymus japonica, as one of the main plant species planted across the city by Beijing city council, was used as the experimental plant. Because all *Euonymus japonicas* were planted by Beijing government, it ensured this study worked with similar homogenous samples. Leaves from one meter height plants of *Euonymus japonica* were collected from different locations, and then stored in ziplock bags and placed in an ice box prior to analysis. Experimental leaf samples were collected from 30 selected sampling locations around the Beijing main road network. Figure 1 shows their geographical distribution.

Spectral Measurements

The reflectance values of the leaves were measured by a spectrometer (Analytical Spectral Devices FieldSpec Pro, ASD 2001) with the Plant Probe (ASD auxiliary product, light source type is Halogen bulb) and the ASD Leaf Clip. The

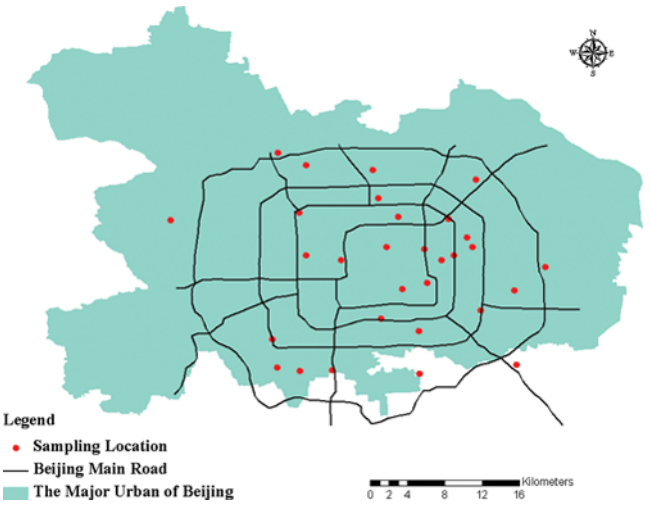

Figure 1. Sampling point distributions across Beijing.

ASD is a single-beam field spectroradiometer with a total of 2100 spectral bands and covering a range of 350–2500 nm (Matson et al. 1994). The spectral measurements were repeated ten times for each leaf. The mean values were taken to represent each leaf's spectral reflectance.

Protein Extraction and SDS-PAGE Analysis

The leaf total protein was extracted and quantified according to Gao et al. (2011) with minor modifications. Approximately 500 mg fresh leaves of each sample were ground into fine power in liquid nitrogen. The grounded tissues were suspended in 5 mL ice-cold 10% w/v trichloroacetic acid/acetone solution containing 0.07% *w/v* dithiothreitol, 1 mM phenylmethanesulfonyl fluoride, and incubated at −20°C for protein precipitation. After centrifugation at 14,000 g for 30 min at 4°C, the supernatant was discarded carefully. The pellet was rinsed for three times with ice-cold acetone containing 0.07% *w/v* dithiothreitol for 15 min at −20°C, and then vacuum-dried and stored at −80°C. A dried pellet of 10 mg was dissolved in 300 μL lysis buffer (7 M urea, 2 M thiourea, 4% *w/v* 3-[(3-cholamidopropyl) dimethylammonio]-1-propanesulfonate and 65 mM dithiothreitol) over 3 h at room temperature. The proteins were harvested by centrifugation at 14,000 g for 15 min at 4°C to remove insoluble materials. The protein concentration was determined with a 2-D Quant Kit (Amersham Bioscience) using bovine serum albumin (2 mg/mL) as the standard. The final concentration of the protein sample was added and adjusted to 2 μg/μL. The 12% sodium dodecyl sulphate-polyacrylamide gel electrophoresis (SDS-PAGE) of leaf soluble proteins was performed according to Laemmli, and 50 μg proteins was loaded for each sample (Laemmli 1970).

Protein Identification and Quantification

In order to study the relationship between spectral reflectance and protein concentration, the specific protein bands that were present in most samples at relatively high concentrations were selected for further tandem mass spectrometry identification and quantification. Selected protein bands were excised from the SDS-PAGE gels and destained with 100 μL of 50% acetonitrile in 50 mM ammonium hydrogen carbonate for approximately 1 h at room temperature. This step was repeated until the gel was colorless. After evaporation of the solvent by vacuum centrifugation, each of the gel plugs was rehydrated with 20 μL of 0.01 mg/mL sequencing-grade modified trypsin (Promega, Madison, WI, USA), and the mixture was agitated at 37°C overnight (16 h). The supernatants were collected, and the gel pieces were rinsed once with 5% trifluoracetic acid in 50% acetonitrile and then twice with 2.5% trifluoracetic acid in 50% acetonitrile. The supernatants were combined and lyophilized. The lyophilized peptides were dissolved in 5 mg/mL CHCA (a-cynao-4-hydroxycinnamic-acid, Sigma, Germany) in 50% acetonitrile and 0.1% trifluoracetic acid.

The mass spectrometry/mass spectrometry experiments for peptide identification were performed using an ultimate high performance liquid chromatography system and a quadrupole time-of-flight mass spectrometer (Waters, Milford, MA) equipped with a nano-electrospray ionization source. The peptides were

subsequently eluted on to an analytical Atlantis C18 column (Waters Corporation) and separated at 1 μL/min with an increasing acetonitrile gradient from 4% to 95% over 50 min. The mobile phase A consisted of 0.1% formic acid in water, and the mobile phase B consisted of 0.1% formic acid in acetonitrile. The mass spectrometer was operated in a positive ion mode with a source temperature of 80°C and a cone gas flow of 10 L/h. The tandem mass spectrometry data were processed with MassLynx version 4.0 software (Waters Corporation) and analyzed with the NCBInr green plant protein sequence database using the Mascot search engine. The following search parameters were used in all of the searches: tolerance of one missed cleavage; and carbamidomethylation and oxidation as the fixed and variable modifications, respectively. A maximum error tolerance of 100 ppm and a 0.3 Da fragment tolerance were allowed. Finally, the protein concentrations in every lane on the 1-D electrophoresis gels were calculated by the specific software Quantity One.

RESULTS AND DISCUSSION

Correlation Between Protein Concentration and Spectral Reflectance

The SDS-PAGE analysis of leaf proteins are shown in Figure 2. Five representative protein bands were selected for further identification by nano-liquid chromatography-mass spectrometry/mass spectrometry. The results showed that A was identified as ATP synthase subunit beta (ATP-SSB), B as ribulose bisphosphate carboxylase (RBC), C as oxygen evolving enhancer protein (OEEP), D as light-harvesting complex II protein (LCP-II), and E as chlorophyll a-b binding protein (Chl-ab). Their sequence coverage was 51.13%, 54.62%, 30.42%, 46.97%, and 100%, respectively.

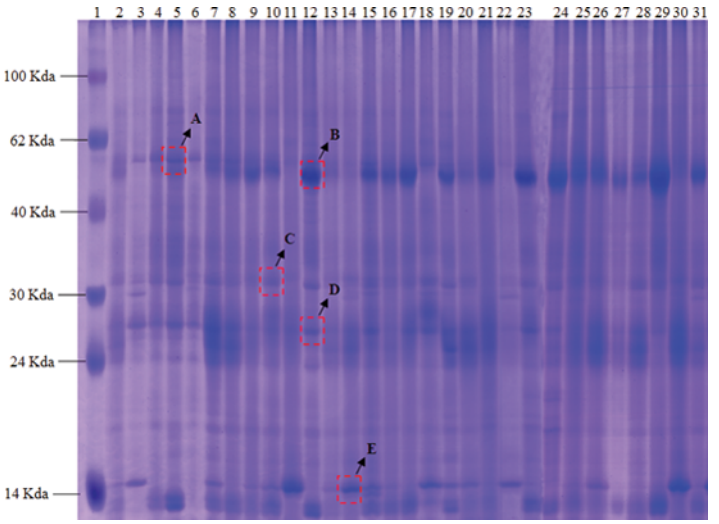

Figure 2. SDS-PAGE analysis of 30 samples. 1: Protein marker (100-14 Kda), A: ATP synthase subunit beta, B: ribulose bisphosphate carboxylase, C: oxygen evolving enhancer protein, D: light-harvesting complex II protein, E: chlorophyll a-b binding protein.

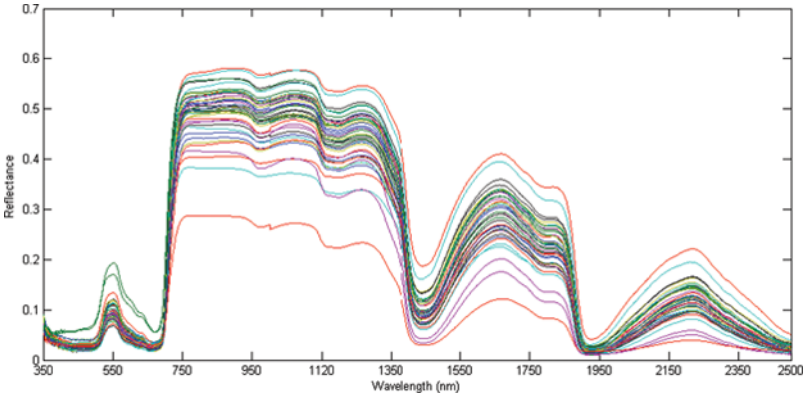

Figure 3. Spectral features of samples.

Figure 3 shows that spectral curves are specific to different leaves. This phenomenon is due to each blade's individual biological characteristics, such as individual chlorophyll sittings (Naidu et al. 2009; VanGaalen, Flanagan, and Peddle 2007). Protein concentration is one indicator of biological characteristics and may relate to the variation of spectral features.

Correlation analysis between protein concentration and spectral reflectance indicated that the correlation coefficient of five proteins had an obviously fluctuation in the 650–750 nm wavelength regions (Figure 4).

The concentration of Chl-ab correlated positively with spectral reflectance in the 350–2500 nm regions and the maximum correlation coefficient ($r = 0.53$, $P = 0.03$) appeared at about 690 nm. This correlation coefficient had a significant decline at 700 nm and was constant above 750 nm. The correlation coefficient of LCP-II was between 0.2 and −0.2, indicating that the concentration had a low correlation with the spectral reflectance. The OEEP, RBC, and ATP-SSB had negative

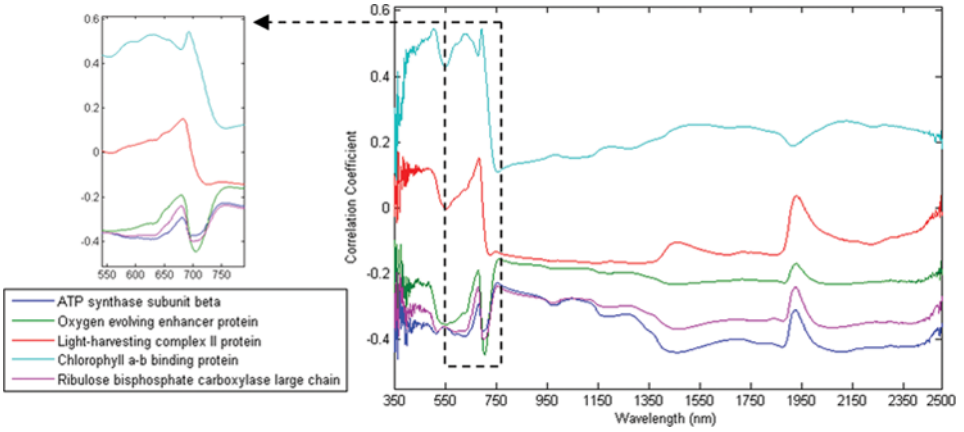

Figure 4. Correlation coefficient between protein concentration and spectral reflectance.

Table 1. Resistant line inspection results

Protein	Left half-slope	Right half-slope	Ratio
RBC	−436153	−569777	1.306
Chl-ab	100111	552967	5.524

correlations with the spectral reflectance. Their minimum correlation coefficients were −0.5, −0.43, and −0.45. In the 650–750 nm regions, the curve trends were nearly identical; first, with an increase followed by a decrease. The maximum negative correlation coefficient value occurred at about 700 nm. This phenomenon may be a result of their molecular weights. The molecular weights of all proteins were greater than 30 kDa, and therefore they can consist of many carbon-hydrogen bonds which can consume energy in process of stretching (Paul and Bhattacharya 2012; Xu et al. 1999; Thut et al. 2008).

Linear and Quadratic Regression Models

This study establishes inversion concentration models of Chl-ab and RBC, the relative concentration of which are larger as shown in Figure 2. Bands of 517 nm and 693 nm were selected to be independent variable because they have a most significant relationships with RBC ($r = -0.43$) and Chl-ab ($r = 0.53$) than the other bands. Before using least squares regression to build a model, Velleman and Hoaglin suggested fitting a resistant line to see if the relationship was linear (Velleman and Hoaglin 1981). This method fits a straight line to the data using a method resistant to outliers. The ratio was close to 1, indicating that the data were linear. The resistant line inspection results (Table 1) showed that RBC is more suitable for the linear model, whereas the Chl-ab binding protein was suitable for the nonlinear model.

Two models were built from the analysis (Figure 5 and Figure 6). RBC (Figure 5) shows a good fit for the linear regression model equation given as follows:

$$f(x) = -448300^{*}\ x + 32050 \tag{1}$$

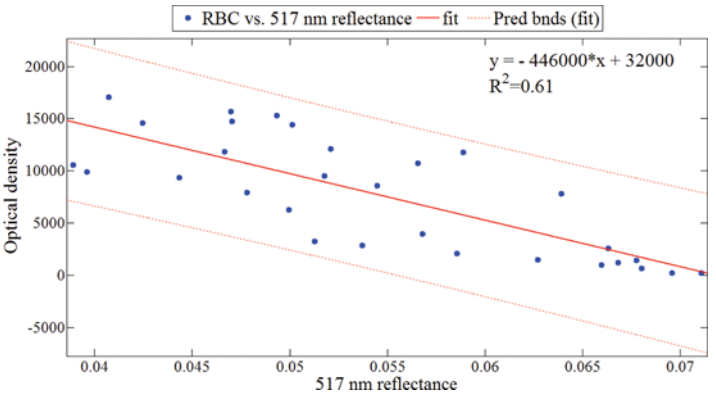

Figure 5. Linear regression inversion for RBC concentration using the 517 nm wavelength.

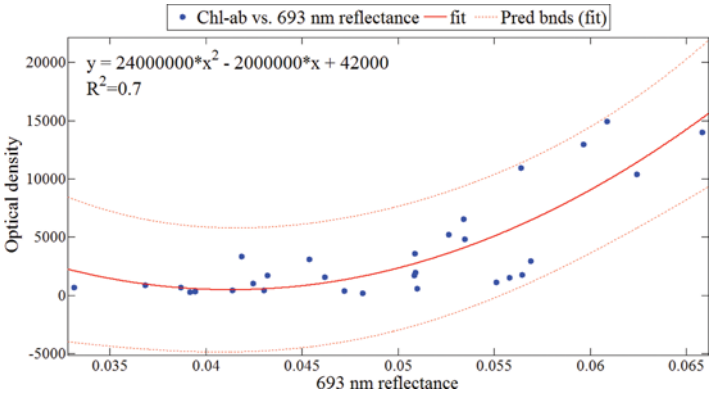

Figure 6. Quadratic regression inversion for Chl-ab concentration using the 693 nm wavelength.

Equation (1) expresses the relationship between RBC concentration and spectral reflectance, where x is spectral reflectance at the wavelength 517 nm, and f(x) is protein's optical density with unit optical density. The R^2 of the model is about 0.61. We used the two-fold method of cross-validation to validate the model, R^2 of train model inversion value, and the test value was 0.6.

In Figure 6, Chl-ab was confirmed to be suitable for the quadratic regression model:

$$f(x) = 10870000^{*}\ x^2 - 775400^{*}\ x + 14650 \tag{2}$$

Equation (2) expresses the relationship between Chl-ab concentration and spectral reflectance, where x is the spectral reflectance at the wavelength 693 nm, and f(x) is protein's optical density with unit optical density. The R^2 of the model is about 0.7. Also, based on two-fold cross-validation method, the R^2 of train model inversion value and test value was 0.55.

Back Propagation (BP) Neutral Networks Model

The aforementioned linear and quadratic regression models provide a quick and simple way to estimate two main types of protein content. However, their accuracies were not very good. Thus, in order to improve the inversion results, a back propagation (BP) neural-network model was established to estimate the protein concentrations. The BP neutral network approach is most widely used because it can be considered as a generalization of the delta rule for nonlinear activation functions and multilayer networks (Ermini, Catani, and Casagli 2005; Pal et al. 2003; Tumbo, Wagner, and Heinemann 2002; Pachepsky, Timlin, and Varallyay 1996). The network of this study was comprised of three layers: an input layer, a middle layer, and an output layer (Figure 7).

Figure 4 shows that correlation coefficient between protein concentration and spectral reflectance varied widely over the wavelength range of 400–750 nm. Thus, this study calculated 17 plant spectral absorption and position parameters (Table 2) and

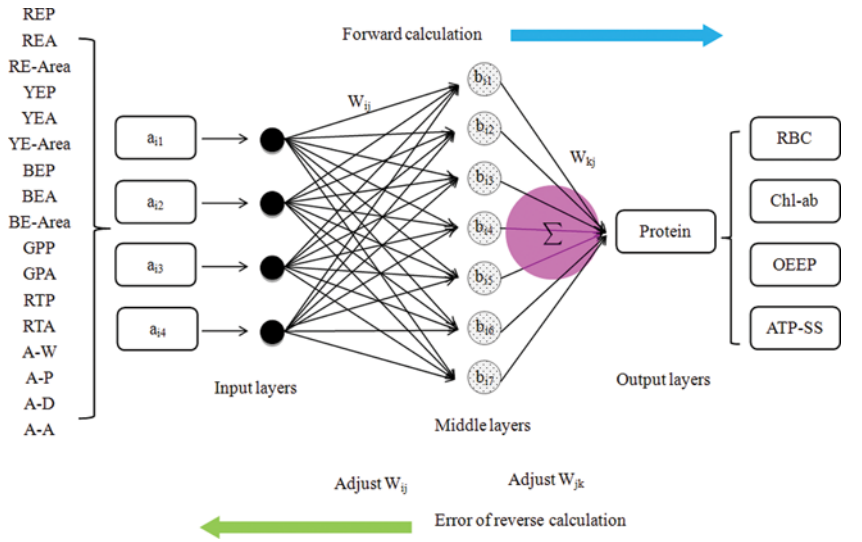

Figure 7. BP neutral network flow chart of protein inversion.

then 4 were used as variables for the input layer (Haboudane et al. 2004; Hansena and Schjoerring 2003; Miller et al. 1991).

The correlation coefficient between the variable and protein concentration was calculated as shown in Table 3. The four biggest correlation coefficients with highly significant level between each protein were selected to use as input variables. To avoid data saturation, the input variables in this model were normalized, based on their possible ranges using the following equation:

$$a_{norm} = (a_i - a_{min})/(a_{mix} - a_{min}) \quad (3)$$

where a_{norm}, a_i, a_{min}, and a_{max} represent the normalized value, the real value input variable, the minimum input variable and the maximum input variable, respectively.

The number of hidden nodes was initially set at seven according to the experience equation (Thiemann and Kaufmann 2000), the learning rate was 0.05, and momentum was 0.03. The epoch size was fixed at 5000. BP Network structure was 4-7-1. Its activation function was {tansig, tansig, purelin} and training algorithm was traindx. REP, YEA, BEA, and GPA were selected as input variables for output variable OEEP. Input variables for ATP-SSB were A-P, A-W, YEA, and RTA; for Chl-ab were BEP, RTA, A-W, and A-P; and for RBC were A-W, A-P, BE-Area, and RTA.

The results of the model are shown in Figure 8. The R^2 results between predicted value and real value (real value is the test data from nano-liquid chromatography-mass spectrometry/mass spectrometry) were 0.90, 0.91, 0.91, and 0.93, corresponding to RBC, Chl-ab, OEEP, and ATP-SSB protein's concentration inversion, respectively. These results also indicated that the model showed stronger correlation and was more precise than the statistical regression model.

Table 2. Plant spectral absorption and position parameters

Variables	Description	Function
Red edge position (REP)	The wavelength with the maximum gradient from 680 to 760 nm.	The indicative character of vegetation stress and leaf senescence.
Red edge amplitude (REA)	The first differential value of the curve of spectrum in red edge position.	Can be as biological and chemical inversion parameters, such predicating chlorophyll and liquid water content.
Red edge area (RE-Area)	The area surrounded by the first derivative from 680 to 760 nm.	Can be calculating nitrogen and chlorophyll content.
Yellow edge position (YEP)	The wavelength with the maximum gradient from 560 to 640 nm.	To analyze leaf-level cell structure and pigment content.
Yellow edge amplitude (YEA)	The first differential value of the curve of spectrum in yellow edge position.	It is well related to pigment content which may be chlorophyll a, chlorophyll b and chlorophyll ab.
Yellow edge area (YE-Area)	The area surrounded by the first derivative from 560 to 640 nm.	Can be used to extract and estimate biophysical and biochemical parameters.
Blue edge position (BEP)	The wavelength with the maximum gradient from 490 to 530 nm.	To estimate vegetation chemical composition, such as protein content.
Blue edge amplitude (BEA)	The first differential value of the curve of spectrum in blue edge position.	To evaluate plant ecological value, leaf structure and protein component.
Blue edge area (BE-Area)	The area surrounded by the first derivative from 490 to 530 nm.	Same as the blue edge amplitude.
Green peak position (GPP)	The wavelength with the maximum reflectance from 510 to 560 nm.	Can be as an index to show vegetation health condition, insect pest and chlorophyll content.
Green peak amplitude (GPA)	Reflectance of the curve of spectrum in green peek position.	It is well correlated to leaf-level chlorophyll content.
Red trough position (RTP)	The wavelength with the minimum reflectance from 650 to 690 nm	Can be determining vegetation macro constituent, such as crude protein.
Red trough amplitude (RTA)	Reflectance of the curve of spectrum in red trough position.	It can be as an index of atmospheric pollution and pigment inversion.
Absorption width (A-W)	The wavelength difference in half of the absorption depth.	To reflect pigment and liquid water content.
Absorption position (A-P)	The wavelength with the minimum reflectance in absorption valley.	It is related to leaf health condition and chlorophyll content.
Absorption depth (A-D)	The depth of the absorption valley.	Same as absorption position.
Absorption area (A-A)	The area of the absorption valley.	Same as absorption position.

Table 3. Correlation coefficients between the spectral variables and protein concentration

Proteins	RBC	Chl-ab	LCP-II	OEEP	ATP-SSB
REP	0.28	−0.45*	0.20	0.58*	0.24
REA	−0.38	0.36	−0.32	−0.36	−0.36
RE-Area	−0.30	0.19	−0.32	−0.16	−0.30
YEP	−0.18	0.39	0.13	0.19	−0.38
YEA	0.13	−0.27	0.13	0.49*	0.42*
YE-Area	−0.40	0.41	−0.17	−0.45*	−0.40
BEP	0.13	−0.49*	−0.16	0.42*	0.12
BEA	−0.35	0.35	−0.17	−0.45*	−0.37
BE-Area	−0.42*	0.46	−0.13	−0.43*	−0.41
GPP	0.13	−0.49*	−0.17	0.42*	0.12
GPA	−0.35	0.35	−0.17	−0.45*	−0.37
RTP	−0.13	−0.11	0.11	0.22	−0.17
RTA	0.45*	−0.57*	−0.17	0.37	0.43*
A-W	0.52*	−0.65*	−0.19	0.43*	0.50*
A-P	−0.64*	0.71*	−0.18	−0.42*	−0.59*
A-D	−0.17	−0.13	−0.33	−0.21	0.16
A-A	0.22	−0.36	−0.34	0.15	0.33

*Represent the significant level at $P < 0.05$ (95% confidence level).

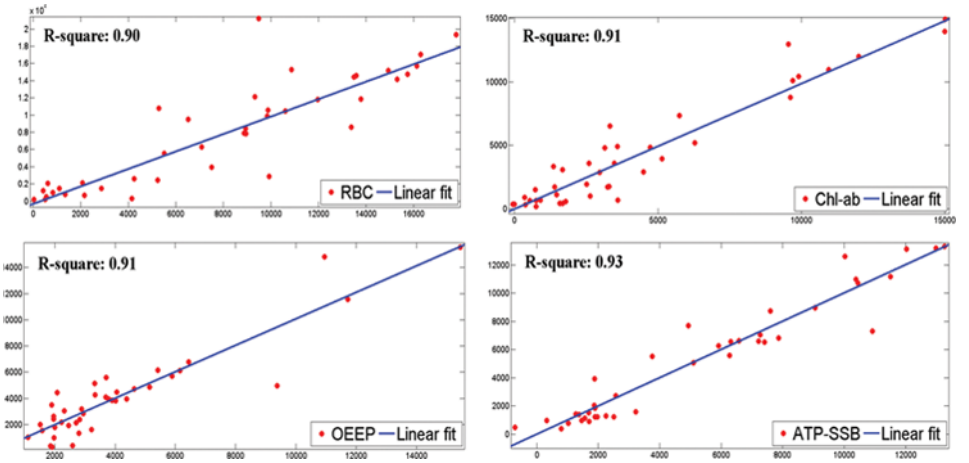

Figure 8. R^2 between predicted value and real value, X axis is real value, Y axis is predicted value.

CONCLUSIONS

This study found that the concentrations of four plant leaf proteins (ATP-SSB, RBC, OEEP, and Chl-ab) in *Euonymus japonica* had a significant relationship with the spectral reflectance in visible spectrum. The linear and quadratic regression models were built to directly obtain the concentrations of two major proteins, RBC and Chl-ab. The experimental results indicated that RBC was more suited for the linear model with 517 nm wavelength and Chl-ab had a good fit for quadratic

regression with the 693 nm wavelength, and their inversion results were acceptable ($R^2 = 0.61$ and 0.7). A more accurate inversion was built by the BP neutral network model using plant spectral absorption and position parameters. This model displayed good results in the concentration inversion of RBC, Chl-ab, OEEP, and ATP-SSB proteins, with better precision than the linear and quadratic regression models. Based on the results obtained from this study, spectral reflectance can provide sufficient information to efficiently detect plant biochemical components to evaluate the health of plants under different environmental conditions. It can be concluded that using spectral reflectance with proper models can predicate plant inner protein concentrations effectively and nondestructively. The linear and quadratic regression models were shown to be simple and rapid, but their accuracy was not satisfactory. The BP neutral network model resulted in precise results, demonstrating the potential to monitor protein concentrations and to be a useful tool for further studies on the effect of environmental pollution on plant health.

FUNDING

The work presented in this paper is supported by Ministry of Science and Technology of China (Project No.: 2012BAJ15B04, 2012AA12A305) and The Hong Kong Polytechnic University (Project No.: 1-ZV4 F, G-U753, G-YK75, G-YJ75).

REFERENCES

Adams, M. L., W. D. Philpot, and W. A. Norvell. 1999. Yellowness index: An application of spectral second derivatives to estimate chlorosis of leaves in stressed vegetation. *Int. J. Remote Sens.* 20: 3663–3675.

Aparicio, N., D. Villegas, J. Casadesus, J. L. Araus, and C. Royo. 2000. Spectral vegetation indices as non-destructive tools for determining durum wheat yield. *Agron. J.* 92: 83–91.

Best, R. G., and J. C. Harlan. 1985. Spectral estimation of green leaf area index of oats. *Remote Sens. Environ.* 17: 27–36.

Blackmer, T. M., J. S. Schepers, and G. E. Vavrel. 1996. Nitrogen deficiency detection using reflected shortwave radiation from irrigated corn canopies. *Agron. J.* 88: 1–5.

Chalke, S. L. 1999. Environmental significance of anthocyanins in plant stress responses. *Photochem. Photobiol.* 70: 1–9.

Curran, P. J., J. L. Dungan, and D. L. Peterson. 2011. Estimating the foliar biochemical concentration of leaves with reflectance spectrometry. *Remote Sens. Environ.* 76: 349–359.

Ermini, L., F. Catani, and N. Casagli. 2005. Artificial neural networks applied to landslide susceptibility assessment. *Geomorphology.* 66: 327–343.

Gao, L., X. Yan, G. Guo, Y. Hu, W. Ma, and Y. Yan. 2011. Proteome analysis of wheat leaf under salt stress by two-dimensional difference gel electrophoresis (2D-DIGE). *Phytochemistry.* 72: 1180–1191.

Haboudane, D., J. R. Miller, E. Pattery, P. J. Zarco-Tejad, and I. B. Strachan. 2004. Hyperspectral vegetation indices and novel algorithms for predicting green LAI of crop canopies: Modeling and validation in the context of precision agriculture. *Remote Sens. Environ.* 90: 337–352.

Harbome, J. B. 1999. The comparative biochemistry of phytoalexin induction in plants. *Biochem. Syst. Ecol.* 27: 335–368.

Hansena, P. M., and J. K. Schjoerring. 2003. Reflectance measurement of canopy biomass and nitrogen status in wheat crops using normalized difference vegetation indices and partial least squares regression. *Remote Sens. Environ.* 86: 542–553.

Hansena, P. M., J. K. Schjoerring, and A. Thomsen. 2002. Prediction grain yield and protein content in winter wheat and spring barley using repeated canopy reflectance measurements and partial least squares regression. *J. Agr. Sci.* 139: 307–318.

Heim, K. E., A. R. Tagliaferro, and D. J. Bobilya. 2002. Flavonoid antioxidants: Chemistry, metabolism and structure-activity relationships. *J. Nutr. Biochem.* 13: 572–584.

Jenneer, C. F., T. D. Ugalde, and D. Aspinall. 1991. The physiology of starch and protein deposition in the endosperm of wheat. *Austr. J. Plant. Phys.* 18: 211–226.

Kalaitzidis, C., S. J. M. Caporn, and M. E. J. Cutler. 2008. Estimating foliar nitrogen concentration of heather (Calluna vulgaris) from Field and Laboratory Spectra. *Water Air. Soil Poll.* 194: 57–66.

Laemmli, U. K. 1970. Cleavage of structural proteins during the assembly of the head of Bacteriophage T4. *Nature.* 227: 680–685.

Markr, R., and C. Loretoc. 2002. FT-NIR Spectroscopic Analysis of Nitrogen in Cotton Leaves. *Appl. Spectrosc.* 56: 1484–1488.

Matson, P., L. F. Johnson, C. Billow, J. Miller, and R. Pu. 1994. Seasonal patterns and remote spectral estimation of canopy chemistry across the Oregon transect. *Ecol. Appl.* 4: 280–298.

Miller, J. R., J. Wu, M. G. Boyer, M. Belanger, and E. W. Hare. 1991. Season patterns in leaf reflectance red edge characteristics. *Int. J. Remote. Sens.* 12: 1509–1523.

Naidu, R. A., E. M. Perry., F. J. Pierce, and T. Mekuria. 2009. The potential of spectral reflectance technique for the detection of Grapevine leafroll-associated virus-3 in two red-berried wine grape cultivars. *Comput. Electron. Agr.* 66: 38–45.

Pachepsky, Y. A., D. Timlin, and G. Varallyay. 1996. Artificial neural networks to estimate soil water retention from easily measurable data. *Soil Sci. Soc. Am. J.* 60: 727–733.

Pal, N. R., S. Pal, J. Das, and K. Majumdar. 2003. SOFM-MLP: A hybrid neural network for atmospheric temperature prediction. *IEEE. T. Geosci. Remote* 41: 2783–2791.

Paul, P., and S. J. Bhattacharya. 2012. Iridium mediated N-H and C-H bond activation of N-(aryl) pyrrole-2-aldimines. Synthesis, structure and, spectral and electrochemical properties. *J. Organomet. Chem.* 713: 72–79.

Sun, Y. L., G. S. Zhuang, W. J. Zhang, Y. Wang, and Y. H. Zhuang. 2006. Characteristics and sources of lead pollution after phasing out leaded gasoline in Beijing. *Atmos. Environ.* 40: 2973–2985.

Thiemann, S., and H. Kaufmann. 2000. Determination of chlorophyll content and trophic state of lakes using field spectrometer and IRS-1C satellite data in the Mecklenburg Lake District, Germany. *Remote Sens. Environ.* 73: 227–235.

Thut, M., C. Manca, C. Tanner, and S. Leutwyler. 2008. Spectral tuning by switching C–H$\cdots$O hydrogen bonds: Rotation-induced spectral shifts of 7-hydroxyquinoline$\cdot$HCOOH isomers. *J. Chem. Phys.* 128: 024304.

Tumbo, S. D., D. G. Wagner, and P. H. Heinemann. 2002. Hyper spectral-based neural network for predicting chlorophyll status in corn. *T. Asae* 45: 825–832.

VanGaalen, K. E., L. B. Flanagan, and D. R. Peddle. 2007. Photosynthesis, chlorophyll fluorescence and spectral reflectance in Sphagnum moss at vary water contents. *Oecologia* 153: 19–28.

Velleman, P. F., and D. C. Hoaglin. 1981. *ABC's of EDA*. California: Duxbury Press.

Wang, T., and S. D. Xie. 2009. Assessment of traffic-related air pollution in the urban streets before and during the 2008 Beijing Olympic Games traffic control period. *Atmos. Environ.* 43: 5682–5690.

Wang, Z. F., L. F. Chen, J. Tao, H. Zhang, and Y. L. Su. 2010. Satellite-based estimation of regional particulate matter (PM) in Beijing using vertical-and-RH correcting method. *Remote Sens. Environ.* 114: 50–63.

Xu, Y. Z., J. Tao, Z. H. Xu, S. F. Weng, J. P. Xu, R. D. Soloway, J. G. Wu, D. F. Xu, and G. X. Xu. 1999. Structural basis for the discrepancy of spectral behavior in C-H stretching band between steroids and long chain hydrocarbon compounds. *Sci. China Ser. B* 42: 178–184.